Non-parametric Data Assimilation Scheme for Land Hydrological Applications

Water Resources Research

RESEARCH ARTICLE
10.1029/2018WR022854

Nonparametric Data Assimilation Scheme for Land Hydrological Applications

M. Khaki[1,2], F. Hamilton[3], E. Forootan[4], I. Hoteit[5], J. Awange[1], and M. Kuhn[1]

[1]School of Earth and Planetary Sciences, Discipline of Spatial Sciences, Curtin University, Perth, Western Australia, Australia, [2]School of Engineering, The University of Newcastle, Callaghan, Australia, [3]Department of Mathematics, North Carolina State University at Raleigh, Raleigh, NC, USA, [4]School of Earth and Ocean Sciences, Cardiff University, Cardiff, UK, [5]Division of Physical Sciences and Engineering, King Abdullah University of Science and Technology, Thuwal, Saudi Arabia

Key Points:
- A nonparametric framework is introduced to improve model estimates
- Kalman-Takens filter is used to integrate GRACE terrestrial water storage (TWS) with model outputs
- The Kalman-Takens filter performed comparable to an adaptive unscented Kalman filter (AUKF) without using model's algorithms

Supporting Information:
- Supporting Information S1

Correspondence to:
M. Khaki,
Mehdi.Khaki@postgrad.curtin.edu.au

Citation:
Khaki, M., Hamilton, F., Forootan, E., Hoteit, I., Awange, J., & Kuhn, M. (2018). Nonparametric data assimilation scheme for land hydrological applications. *Water Resources Research*, *54*. https://doi.org/10.1029/2018WR022854

Received 28 FEB 2018
Accepted 12 JUN 2018
Accepted article online 19 JUN 2018

Abstract Data assimilation, which relies on explicit knowledge of dynamical models, is a well-known approach that addresses models' limitations due to various reasons, such as errors in input and forcing data sets. This approach, however, requires intensive computational efforts, especially for high-dimensional systems such as distributed hydrological models. Alternatively, data-driven methods offer comparable solutions when the physics underlying the models are unknown. For the first time in a hydrological context, a nonparametric framework is implemented here to improve model estimates using available observations. This method uses Takens delay coordinate method to reconstruct the dynamics of the system within a Kalman filtering framework, called the Kalman-Takens filter. A synthetic experiment is undertaken to fully investigate the capability of the proposed method by comparing its performance with that of a standard assimilation framework based on an adaptive unscented Kalman filter (AUKF). Furthermore, using terrestrial water storage (TWS) estimates obtained from the Gravity Recovery And Climate Experiment mission, both filters are applied to a real case scenario to update different water storages over Australia. In situ groundwater and soil moisture measurements within Australia are used to further evaluate the results. The Kalman-Takens filter successfully improves the estimated water storages at levels comparable to the AUKF results, with an average root-mean-square error reduction of 37.30% for groundwater and 12.11% for soil moisture estimates. Additionally, the Kalman-Takens filter, while reducing estimation complexities, requires a fraction of the computational time, that is, ~8 times faster compared to the AUKF approach.

1. Introduction

A precise study of terrestrial water storage (TWS) changes is essential to better understand the spatiotemporal variations of water resources and their effects on the hydrological cycles. In this regard, hydrological models become valuable tools for simulating hydrological processes at global (e.g., Coumou & Rahmstorf, 2012; Döll et al., 2003; Huntington, 2006; van Dijk et al., 2013) and regional (e.g., Chiew et al., 1993; Christiansen et al., 2007; Huang et al., 2016; Wooldridge & Kalma, 2001) scales. These models are formulated based on physical/conceptual principles to represent *reality* and are still being developed to accurately simulate all complex hydrological processes, including interactions between water cycle components (e.g., surface and subsurface water exchange). These models, however, can be subject to various sources of uncertainties, for example, errors in input and forcing data, and imperfect accounting for the physical underlying dynamics, such as those used to simulate evapotranspiration (van Dijk et al., 2011; Vrugt et al., 2013).

Classically, data assimilation can be used to improve imperfect models by integrating available observations with the underlying physical model. Many studies have implemented data assimilation techniques in the fields of ocean and atmospheric sciences (e.g., Bennett, 2002; Hoteit et al., 2002, 2012; Kalnay, 2003; Schunk et al., 2004; Lahoz et al., 2007; Tardif et al., 2015; Zhang et al., 2012; Zhao et al., 2017) and hydrology (e.g., Girotto et al., 2016, 2017; Kumar et al., 2016; Rasmussen et al., 2015; Schumacher et al., 2018; Seo et al., 2003; Vrugt et al., 2005; Weerts & El Serafy, 2006). Data assimilation is often used to improve model simulations of soil moisture (e.g., Brocca et al., 2010; Calvet et al., 1998; Entekhabi et al., 1994; Kumar et al., 2009, 2015; De Lannoy, Reichle, Houser, et al. (2007); De Lannoy et al., 2009, 2015; Lievens et al., 2015; Montaldo et al., 2001; Reichle et al., 2002; Renzullo et al., 2014), TWS (e.g., Khaki, Hoteit, et al., 2017; Khaki, Forootan, Kuhn, Awange,

Papa, & Shum, 2018; Khaki, Forootan, Kuhn, Awange, van Dijk, et al., 2018; Schumacher et al., 2016, 2018; Tangdamrongsub et al., 2015; van Dijk et al., 2014; Zaitchik et al., 2008), evapotranspiration and sensible heat fluxes (e.g., Irmak & Kamble, 2009; Jian et al., 2014; Pipunic et al., 2008; Schuurmans et al., 2003), and surface water and river discharge (e.g., Andreadis et al., 2007; Awwad et al., 1994; Bras & Restrepo-Posada, 1980; Giustarini et al., 2011; Lee et al., 2011; Li et al., 2015; Madsen & Skotner, 2005; McMillan et al., 2013; Neal et al., 2009; Vrugt et al., 2006; Young, 2002). Standard data assimilation techniques have their limitations though, for example, the general requirement of intensive computations for high-dimensional systems in realistic applications (Tandeo et al., 2015). Furthermore, when a physical model (i.e., model's underlying equations) is not available, the application of a traditional data assimilation framework that relies on these equations for forecasting can be limited (see, e.g., Arnold et al., 2013; Hersbach et al., 2007; Palmer, 2001; Reichle & Koster, 2005).

A number of studies employ data-driven (nonparametric) approaches to produce accurate statistical simulations (e.g., Dreano et al., 2015; Hamilton et al., 2016; Lguensat et al., 2017; Sauer, 2004; Tandeo et al., 2015). Hamilton et al. (2015) and Berry and Harlim (2016) considered the case when models are partially known. In other cases with completely unknown systems, for example, no available information about the physics of the underlying models and correspondingly their equations, the application of data assimilation becomes rather complicated. Hamilton et al. (2016) developed a new model-free filter based on the nonparametric Takens approach and Kalman filtering when the physical model is not available. The main idea of Takens' theorem is that the model equations can be replaced by a data-driven nonparametric reconstruction of the system's dynamics. The filter implements Takens' method for attractor reconstruction within the Kalman filtering framework, allowing for a model-free approach to filter noisy data (Hamilton et al., 2016). Takens method has been used in various studies for nonparametric time series predictions (see, e.g., Packard et al., 1980; Sauer et al., 1991, 2004; Takens, 1981). This technique replaced the model with a delay coordinate embedding scheme and has been shown by Hamilton et al. (2016) to not only obtain comparable results to a standard Kalman filter-based framework but also may perform better when model errors are significant. A similar idea has been used by Tandeo et al. (2015) and Lguensat et al. (2017) to simulate the dynamics of complex systems using a nonparametric sampler. They applied an Analog Data Assimilation scheme that reconstructs the system's dynamics in a fully data-driven manner. While Analog Data Assimilation does not require knowledge of the dynamical model, it assumes that a representative catalog of trajectories of the system is available. They show that the data-driven method performs well without using the physical model.

The main motivation of this study, therefore, is to apply for the first time the Kalman-Takens method in a hydrological context and investigate its capability to enhance a hydrological model's estimates (Figure 1). Its performance is then compared with that of a traditional data assimilation system. The motivation behind selecting the Kalman-Takens method is that it does not use the model's equations and requires less computational burden to predict high-dimensional systems compared to other existing methods (e.g., Berry & Harlim, 2016; Hamilton et al., 2015; Tandeo et al., 2015). This study extends the Kalman-Takens approach to enable its application to a more complicated state observation transition systems, for example, for a case of updating various variables (e.g., soil moisture and groundwater) using only TWS observations. The proposed scheme exploits model trajectories for these variables as the training data and is then applied to assimilate TWS data derived from the Gravity Recovery And Climate Experiment (GRACE) satellite mission into the hydrological system states over Australia for the period 2003–2013. It should be pointed out here that the use of model trajectory in this method, and the reliance of data-driven methods on data in general results in updating observable state variables only. This, however, is different in a standard data assimilation, which can further update other variables subject to availability of the physical model.

GRACE TWS data have been assimilated in many studies, where they have proved to be highly capable of improving the performance of hydrological models (e.g., Eicker et al., 2014; Reager et al., 2015; Schumacher et al., 2018; van Dijk et al., 2014; Zaitchik et al., 2008). Nevertheless, GRACE data assimilation has always been challenging due to the unique characteristics of its measurements, such as the coarser spatiotemporal resolution compared to most of the existing hydrological models (Khaki, Schumacher, et al., 2017). A successful data assimilation method should be able to account for these limitations in GRACE products while vertically spreading their information into various water compartments (see, e.g., Khaki, Schumacher, et al., 2017; Schumacher et al., 2016). Khaki, Hoteit, et al. (2017) showed that assimilating GRACE data can significantly improve the hydrological model performance over Australia (see also Khaki, Ait-El-Fquih, et al, 2017; Tian et al., 2017). In order to benchmark the performance of the proposed data-driven technique, its outputs are compared to those of a standard data assimilation framework based on an adaptive unscented Kalman filter (AUKF; Berry

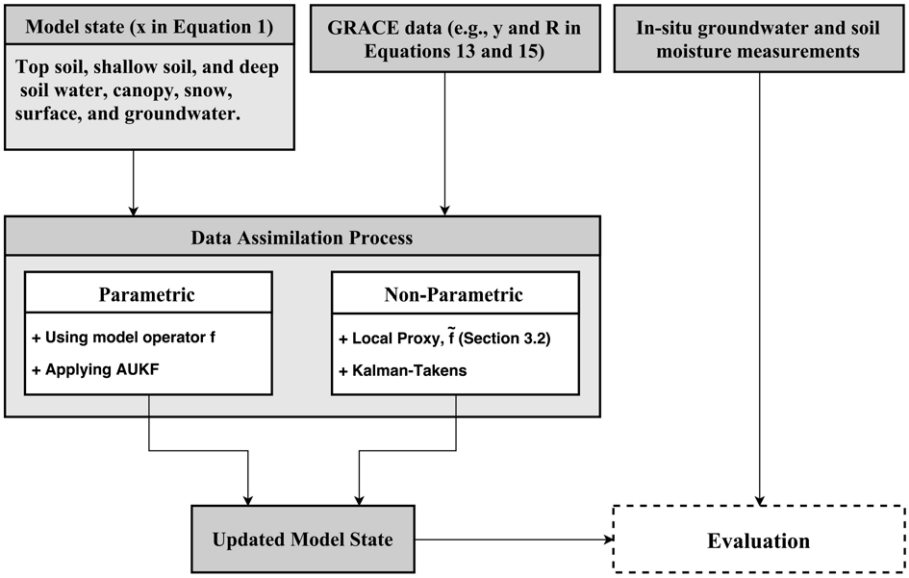

Figure 1. A schematic illustration of the data integration process implemented for this study.

& Sauer, 2013). The results of both methods are evaluated against in situ measurements, as well as through a synthetic experiment to fully investigate their efficiency in assimilating GRACE TWS data.

The remainder of this contribution is organized as follows: data sets are presented in section 2, the filtering scheme described in section 3, and the results discussed in section 4 before concluding the study in section 5.

2. Model and Data

2.1. World-Wide Water Resources Assessment

The $1° \times 1°$ version of the World-Wide Water Resources Assessment (W3RA; http://www.wenfo.org/wald/data-software/) model from the Commonwealth Scientific and Industrial Research Organisation is chosen for the study. The model is designed to simulate landscape water stores and describe the water balance of the soil, groundwater, and surface water stores in which each cell is modeled independently of its neighbors (Renzullo et al., 2014; van Dijk, 2010). The model's forcing includes daily meteorological fields of minimum and maximum temperature, shortwave radiation, and precipitation from Princeton University (Sheffield et al., 2006). The model state vector in our experiment is composed of storages of the top, shallow root, and deep root soil layers, groundwater, and surface water for the period of January 2003 to December 2012.

2.2. Gravity Recovery And Climate Experiment Terrestrial Water Storage

For the same period, GRACE level 2 (L2) Stokes' coefficients (up to degree and order 90) and associated full error information are obtained from the ITSG-Grace2014 gravity field model (Mayer-Gürr et al., 2014). Three degree 1 coefficients (C10, C11, and S11) and degree 2 and order 0 (C20) coefficient are replaced by those of Swenson et al. (2008) and that of Cheng and Tapley (2004), respectively. Further, we apply the DDK2 smoothing filter (Kusche et al., 2009) to mitigate a colored/correlated noise in the coefficients (see also Khaki, Forootan, Kuhn, Awange, Longuevergne, & Wada, 2018), and thereafter convert them into $1° \times 1°$ TWS fields following Wahr et al. (1998). The mean TWS for the study period is taken from the W3RA model and is aggregated to the GRACE TWS change time series to reach absolute values related to W3RA (Zaitchik et al., 2008). Error information of ITSG-Grace2014 is used to construct an observation error covariance matrix (Eicker et al., 2014; Schumacher et al., 2016).

2.3. In Situ Measurements

In situ groundwater and soil moisture measurements are used to evaluate the performance of the proposed data assimilation framework. Groundwater data are provided from the New South Wales Government within the Murray-Darling Basin, which includes 70% of Australia's irrigated area, covers an area of over 1×10^6 km^2 and extends over much of the central and southeastern parts of Australia (Mercer et al., 2007). The data are rescaled to a monthly temporal scale to be consistent with GRACE and time series of groundwater storage

anomalies. Considering that a specific yield for converting well water levels to variations in groundwater storage (Rodell et al., 2007; Zaitchik et al., 2008) is not available, we use the value of 0.13 specific yield obtained from the range between 0.115 and 0.2 as suggested by the Australian Bureau of Meteorology and Seoane et al. (2013).

Furthermore, in situ soil moisture products are acquired from the moisture-monitoring network, known as the OzNet network (http://www.oznet.org.au/), over the Murrumbidgee catchment (Smith et al., 2011) and rescaled to the same temporal scale as above. The data contain long-term records of measured volumetric soil moisture at various soil depths at 57 locations across the Murrumbidgee catchment area. Soil measurements at 0–8, 0–30, and 0–90 cm layers are used to assess the estimated soil moisture results of the proposed assimilation framework. The results can be evaluated using representative soil moisture sites within the basin. Here we use an analysis suggested by De Lannoy, Pauwels, et al. (2007) to acquire the representative soil moisture in situ measurements (see other methods in, e.g., Famiglietti et al., 2008; Orlowsky & Seneviratne, 2014; Nicolai-Shaw et al., 2015). The method is based on relative differences $d_{m,n}$ for site m and time step n, which can be calculated as (De Lannoy, Pauwels, et al., 2007)

$$d_{m,n} = \frac{SM_{m,n} - \overline{SM}_n}{\overline{SM}_n}, \tag{1}$$

where $SM_{m,n}$ is the soil moisture measurement at m and n, and $\overline{SM}_n$ represents the spatially averaged soil moisture. Once $d_{m,n}$ is calculated for each site, the temporally average difference ($\bar{d}_m$) and its standard deviation ($STD(d_m)$) are computed. The most representative site is then the one with $\bar{d}_m$ and $STD(d_m)$ closer to 0.

3. Methodology

3.1. Adaptive Unscented Kalman Filter

Consider the following nonlinear system,

$$\mathbf{x}_t = \mathbf{f}(\mathbf{x}_{t-1}) + \mathbf{v}_{t-1}, \tag{2}$$

$$\mathbf{y}_t = \mathbf{h}(\mathbf{x}_t) + \mathbf{u}_t, \tag{3}$$

where $\mathbf{f}$, the system dynamics, describes the evolution of state vector, $\mathbf{x}$, over time (t) and $\mathbf{h}$, the observation function, maps $\mathbf{x}_t$ to the observations, $\mathbf{y}_t$. $\mathbf{v}_{t-1}$ represent the process noise, which is assumed to be Gaussian with mean 0 and covariance $\mathbf{Q}$. $\mathbf{u}_t$ indicates observation noise with covariance $\mathbf{R}$, which is assumed to be known (see section 2). In the present study, $\mathbf{x}$ consists of different water storages including top, shallow and deep soil water, vegetation, snow, surface, and groundwater storages, while $\mathbf{y}$ represents the GRACE TWS data.

For nonlinear systems, the unscented Kalman filter (UKF) (Julier & Uhlmann, 1997, 2004; Julier et al., 2000; Simon, 2006; Wan & van der Merwe, 2001; Terejanu, 2009) can be used for state estimation. The UKF approximates the propagation of the mean and covariance of a random variable through a nonlinear function using a deterministic sampling approach that generates an ensemble of state values known as sigma points. Given the current state and covariance estimates $\mathbf{x}^a_{t-1}$ and $\mathbf{P}^a_{t-1}$ at step t of the filter, $2L + 1$ sigma points (where L is the dimension of the state vector) are generated by

$$\mathbf{x}^0_{t-1} = \mathbf{x}^a_{t-1}, \tag{4}$$

$$\mathbf{x}^i_{t-1} = \mathbf{x}^a_{t-1} + \left(\sqrt{(L+\lambda)\mathbf{P}^a_{t-1}}\right)_i \quad i = 1, \ldots, L, \tag{5}$$

$$\mathbf{x}^{i+L}_{t-1} = \mathbf{x}^a_{t-1} - \left(\sqrt{(L+\lambda)\mathbf{P}^a_{t-1}}\right)_i \quad i = 1, \ldots, L, \tag{6}$$

with $\left(\sqrt{(L+\lambda)\mathbf{P}^a_{t-1}}\right)_i$ being the ith column of the matrix square root (e.g., lower triangular Cholesky factorization; Wan & van der Merwe, 2000) of $(L+\lambda)\mathbf{P}^a_{t-1}$. The corresponding weights to the above sigma points defined as

$$w^0_s = \frac{\lambda}{(L+\lambda)}, \tag{7}$$

$$w_c^0 = \frac{\lambda}{(L+\lambda)} + (1 - \alpha^2 + \beta), \tag{8}$$

$$w_s^i = w_c^i = \frac{1}{2(L+\lambda)} \quad i = 1, \ldots, 2L, \tag{9}$$

where $\sum_{i=0}^{2L} w_s^i = \sum_{i=0}^{2L} w_c^i = 1$. In equations (5)–(9), λ is the scaling parameter, which can be calculated as $\lambda = \alpha^2(L + \kappa) - L$. The scaling factor α determines the spread of the sigma points around $\mathbf{x}_{t-1}^a$, and κ is a secondary scaling parameter usually set to 0 (the specific value of kappa is not critical; see e.g., Julier & Uhlmann, 1997; Van der Merwe, 2004). The β is employed to incorporate a prior knowledge about the noise distribution (e.g., the optimal choice for Gaussian distribution is $\beta = 2$; e.g., Wan & van der Merwe, 2001).

Between these factors, the selection of α has larger impacts on the ensemble spreads and controls the *size* of the sigma point distribution. The α determines how the sigma points can be scaled toward or away from the mean of the prior distribution. For example, $\alpha = 1$ and correspondingly $\lambda = 0$ leads the distance between $\mathbf{x}_{t-1}^a$ and the sigma points to be proportional to $\sqrt{L}$. Positive values of λ (for $\alpha > 1$) scales the sigma points further from $\mathbf{x}_{t-1}^a$, while negative values of λ (for $\alpha < 1$) scale the sigma points toward $\mathbf{x}_{t-1}^a$. In other words, the larger values for this scaling factor cause a larger spread in the sigma points while smaller values result in more concentration around prior distribution (Van der Merwe, 2004). Ideally, α should be a small number, for example, $1e-4 \leq \alpha \leq 1$ (Song & He, 2009) to avoid sampling nonlocal effects when the nonlinearities are strong. However, optimal sets of this factor along with κ and β are generally problem specific and can be optimized arbitrarily. For the current study, the values of parameters are assumed as $\alpha = 0.5$, $\kappa = 0$, and $\beta = 2$. Nevertheless, it is found that the implemented AUKF is not very sensitive to the parameter selection as long as they result in a numerically well-behaved set of sigma points and weights (see also ; Van der Merwe, 2004).

The sigma points are advanced forward one time step using model **f** and observed using the function **h**,

$$\mathbf{x}_t^{f,j} = \mathbf{f}(\mathbf{x}_{t-1}^j), \quad j = 0, \ldots, 2L, \tag{10}$$

$$\mathbf{y}_t^{f,j} = \mathbf{h}(\mathbf{x}_t^{f,j}), \quad j = 0, \ldots, 2L. \tag{11}$$

The transformed points ($\mathbf{x}_t^{f,j}$ and $\mathbf{y}_t^{f,j}$) are then used to calculate their respective forecast means and covariance matrices,

$$\mathbf{x}_t^f = \sum_{j=0}^{2L} w_s^j \mathbf{x}_t^{f,j}, \tag{12}$$

$$\mathbf{y}_t^f = \sum_{j=0}^{2L} w_s^j \mathbf{y}_t^{f,j}, \tag{13}$$

$$\mathbf{P}_t^f = \sum_{j=0}^{2L} w_c^j \left(\mathbf{x}_t^{f,j} - \mathbf{x}_t^f\right)\left(\mathbf{x}_t^{f,j} - \mathbf{x}_t^f\right)^T + \mathbf{Q}_{t-1}, \tag{14}$$

$$\mathbf{P}_{\mathbf{y}_t^f} = \sum_{j=0}^{2L} w_c^j \left(\mathbf{y}_t^{f,j} - \mathbf{y}_t^f\right)\left(\mathbf{y}_t^{f,j} - \mathbf{y}_t^f\right)^T + \mathbf{R}_t, \tag{15}$$

as well as the cross covariance between $\mathbf{x}_t^f$ and $\mathbf{y}_t^f$,

$$\mathbf{P}_{\mathbf{x}_t^f, \mathbf{y}_t^f} = \sum_{j=0}^{2L} w_c^j \left(\mathbf{x}_t^{f,j} - \mathbf{x}_t^f\right)\left(\mathbf{y}_t^{f,j} - \mathbf{y}_t^f\right)^T. \tag{16}$$

In the analysis step of the filter, the measurements (e.g., GRACE-derived TWS) are used to correct the forecasted state and respective covariance matrix using the Kalman update equations,

$$\mathbf{x}_t^a = \mathbf{x}_t^f + \mathbf{K}(\mathbf{y}_t - \mathbf{y}_t^f), \tag{17}$$

$$\mathbf{K} = \mathbf{P}_{\mathbf{x}_t^f,\mathbf{y}_t^f}\mathbf{P}_{\mathbf{y}_t^f}^{-1}, \tag{18}$$

$$\mathbf{P}_t^a = \mathbf{P}_{\mathbf{x}_t^f} - \mathbf{K}\mathbf{P}_{\mathbf{y}_t^f}\mathbf{K}^T. \tag{19}$$

where **K** is the Kalman gain.

Critical to the success of the UKF is the selection of the filter noise covariances and in particular the process noise covariance matrix **Q**. Here we use the method of Berry and Sauer (2013) to adaptively estimate this covariance matrix. We refer to this as the *AUKF*. Building on the method of Mehra, (1970, 1972), the general idea of Berry and Sauer (2013) is to use the increment, $\epsilon_t = \mathbf{y}_t - \mathbf{y}_t^f$, to estimate the noise covariance at each time step. The method begins by forming an empirical estimate $\mathbf{Q}_{t-1}^e$ for **Q**,

$$\mathbf{P}_{t-1}^e = \mathbf{F}_{t-1}^{-1}\mathbf{H}_{t-1}^{-1}\epsilon_{t-1}\epsilon_{t-1}^T\mathbf{H}_{t-1}^{-T} + \mathbf{K}_{t-1}\epsilon_{t-1}\epsilon_{t-1}^T\mathbf{H}_{t-1}^{-T}, \tag{20}$$

$$\mathbf{Q}_{t-1}^e = \mathbf{P}_{t-1}^e - \mathbf{F}_{t-2}\mathbf{P}_{t-2}^a\mathbf{F}_{t-2}^T, \tag{21}$$

where $\mathbf{P}_{t-1}^e$ is an empirical estimate of the background covariance. In equations (20) and (21), **F** and **H** are local linearizations of the nonlinear dynamic models **f** and **h**, respectively, and are estimated using a linear regression on the ensembles (see equation 7 in ; Berry & Sauer, 2013, for details regarding this linearization). It is worth mentioning that we must store linearizations $\mathbf{F}_{t-2}, \mathbf{F}_{t-1}, \mathbf{H}_{t-1}, \mathbf{H}_t$, increments $\epsilon_{t-1}, \epsilon_t$, analysis covariance $\mathbf{P}_{t-2}^a$, and Kalman gain $\mathbf{K}_{t-1}$ from the $t-1$ and $t-2$ steps of the filter. To form a stable estimate of **Q**, the noisy estimate $\mathbf{Q}_{t-1}^e$ is combined using an exponentially weighted moving average,

$$\mathbf{Q}_t = \mathbf{Q}_{t-1} + (\mathbf{Q}_{t-1}^e - \mathbf{Q}_{t-1})/\tau, \tag{22}$$

where τ is the window of the moving average. Berry and Sauer (2013) & Hamilton et al. (2016) provide additional details on the estimation of noise covariance.

3.2. Kalman-Takens Method

The main idea of the Kalman-Takens method is to replace the model-based forecast in the AUKF with the advancement of the dynamics nonparametrically, thus requiring no knowledge of **f** (in equation (2). We provide a brief description of the method below, specifically highlighting modifications in adopting the algorithm to our problem. Full details of the methodology can be found in Hamilton et al., (2016, 2017).

In the present study, we consider a different setup to implement the Kalman-Takens filter for a more complicated state observation transition systems. While the data available are gridded GRACE TWS, our interest is in estimating the different water variables (i.e., top, shallow and deep soil water, vegetation, snow, surface, and groundwater). These variables with no independent observation available are provided by the W3RA model and are used to produce delay coordinate vectors. We generate a synthetic set of model trajectories (open-loop run) for these variables to serve as the training data for the Kalman-Takens filter. The training data represent the state of the system. It is also used to generate a local proxy $\tilde{\mathbf{f}}$ for the unknown model **f** (cf. equation (2), which is not available in the nonparametric framework, so equation (10) for advancing the ensemble forward in time in AUKF is not implementable. This brings us to equation (23), which defines the delay coordinate vector **z** at each step of the filter using the historical state variables from the open-loop run by

$$\mathbf{z}_t = [\mathbf{x}^o{}_t, \mathbf{x}^o{}_{t-1}, \ldots, \mathbf{x}^o{}_{t-d}], \tag{23}$$

where d is the number of temporal delays. $\mathbf{x^o}$ contains the open-loop top, shallow and deep soil moisture, vegetation, snow, surface, and groundwater. Once the delay coordinate is created, the assimilation procedure can be applied. At each AUKF step, an ensemble of delay vectors is formed and advanced nonparametrically using a local approximation $\tilde{\mathbf{f}}$. This nonparametric prediction helps to build local models for predicting the dynamics at the forecast step (Hamilton et al., 2017). Given the above current delay coordinate, the nonparametric advancement starts by locating the N nearest neighbors (i.e., points located within a given Euclidean distance; not only adjacent points), within a set of training data,

$$\begin{aligned}\mathbf{z}_t^1 &= \left[\mathbf{x}^{o1}{}_t, \mathbf{x}^{o1}{}_{t-1}, \ldots, \mathbf{x}^{o1}{}_{t-d}\right],\\ \mathbf{z}_t^2 &= \left[\mathbf{x}^{o2}{}_t, \mathbf{x}^{o2}{}_{t-1}, \ldots, \mathbf{x}^{o2}{}_{t-d}\right],\\ &\vdots\\ \mathbf{z}_t^N &= \left[\mathbf{x}^{oN}{}_t, \mathbf{x}^{oN}{}_{t-1}, \ldots, \mathbf{x}^{oN}{}_{t-d}\right].\end{aligned} \tag{24}$$

The known $\mathbf{z}_{t+1}^1, \mathbf{z}_{t+1}^2, \ldots, \mathbf{z}_{t+1}^N$ (based on $\mathbf{x}^{o1}{}_{t+1}, \mathbf{x}^{o2}{}_{t+1}, \ldots, \mathbf{x}^{oN}{}_{t+1}$), are used in a local model to predict $\mathbf{z}_{t+1}$. The local model $\tilde{\mathbf{f}}$, which can be generated using a weighted average of the nearest neighbors (Hamilton et al., 2016; Lagergren et al., 2018) can be written as,

$$\mathbf{z}_{t+1} = \omega_1 \mathbf{z}_{t+1}^1 + \omega_2 \mathbf{z}_{t+1}^2 + \ldots + \omega_N \mathbf{z}_{t+1}^N, \tag{25}$$

$$\omega_i = \frac{e^{-(d_i/\sigma)^2}}{\sum_{j=1}^{N} e^{-(d_j/\sigma)^2}}, \tag{26}$$

where d_i is the distance of the jth neighbor to $\mathbf{z}_t$ and σ is a bandwidth parameter, which controls the contribution of each neighbor in the local model (here $\sigma = 2$). The above prediction is applied to estimate the delay coordinate vector at $t + 1$.

The process of building a local model for forecasting the delay coordinate vector is repeated for each sigma point in the ensemble. After $\tilde{\mathbf{f}}$ has been defined, the remainder of the AUKF update scheme is implemented. Important to the Kalman-Takens method is the selection of d (the number of delays) and neighbors N. Here we consider different values of N and d and set them based on the filter performance, which is described in section 4. The assumption of using the model trajectory rather than observations for generating delay vectors allows us to reconstruct the system representing various water storage compartments. The same assumption is made by Lguensat et al. (2017), where trajectories of the system and not the physical model are available. In fact, we hypothesize that the available model outcomes can be used for the nonparametric sampling of the dynamics and updated by the GRACE TWS (as a summation of all the water variables at each grid point). This means that one can essentially correct state variables of the system, without having data for each individually, using the data-driven framework. The application of this method can address some severe limitations in traditional data assimilation such as large computational cost.

3.3. Synthetic Experiment

A synthetic experiment is undertaken to assess the efficiency of the proposed data assimilation schemes in simulating physical processes. One important problem with hydrological models, and specifically W3RA, is their limitations in simulating anthropogenic impacts on the water cycle. For example, excessive groundwater extractions, which can largely affect subsurface water storages, are not modeled in W3RA and a successful data assimilation process should be able to correct for this drawback by taking the advantage of additional observations. Here we choose to test both AUKF and Kalman-Takens filters to improve upon model simulations between 2003 and 2013 over Iran (32.4279°N, 53.6880°E). The rationale behind choosing Iran for this synthetic analysis, and not Australia, is that a remarkable water storage decline is reported over this region, mainly due to anthropogenic impacts, which cannot be detected by W3RA (see Khaki, Forootan, Kuhn, Awange, van Dijk, et al., 2018). A major part of the negative water storage trend is due to human impacts (see details in ; Forootan et al., 2017; Khaki, Forootan, Kuhn, Awange, van Dijk, et al., 2018). Synthetic observations are produced using the WaterGAP Global Hydrology Model (WGHM; Döll et al., 2003; Müller Schmied et al., 2014) monthly TWS outputs, which contain the anthropogenic impacts (Khaki, Forootan, Kuhn, Awange, van Dijk, et al., 2018), at two different spatial resolution of $1° \times 1°$ and $3° \times 3°$. This can help to test whether data assimilation can account for human impacts on water storage and also to investigate the effect of spatial resolution on the final results. WGHM TWS estimates are assumed as our observations after rescaling into $1° \times 1°$ and $3° \times 3°$ and perturbing using Monte Carlo sampling of multivariate normal distributions with the errors representing the GRACE level 2's standard errors. The data assimilation is implemented using both filtering methods at the aforementioned spatial scales.

3.4. Evaluation Metrics

To evaluate the assimilation results against in situ groundwater and soil moisture measurements, three metrics, (i) the root-mean-square errors (RMSE), (ii) standard deviation (STD), and (iii) Nash-Sutcliffe coefficient

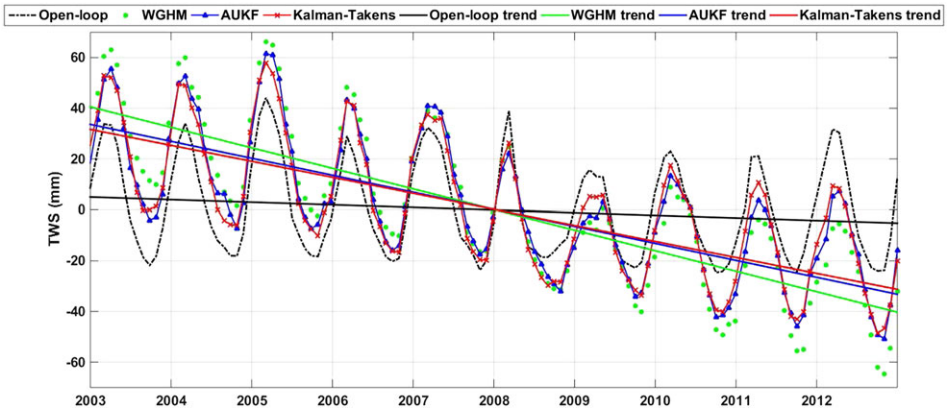

Figure 2. Average TWS variation time series over Iran from AUKF, Kalman-Takens, open-loop run, and WGHM with corresponding trend lines. TWS = terrestrial water storage.

(NSE) are used. Groundwater and soil moisture in situ measurements from various stations are spatially averaged to the location of the nearest model grid points and are compared with their respective estimates. To this end, using the variation time series of in situ data and the results of assimilation techniques, RMSE, STD, and NSE are calculated by

$$RMSE = \sqrt{\frac{1}{n}\sum_{i=1}^{n}(x_i - z_i)^2}, \tag{27}$$

$$STD = \sqrt{\frac{1}{n}\sum_{i=1}^{n}(x_i - \bar{x})^2}, \tag{28}$$

$$NSE = 1 - \left[\frac{\sum_{i=1}^{n}(x_i - z_i)^2}{\sum_{i=1}^{n}(z_i - \bar{z})^2}\right], \tag{29}$$

where x_i is the predicted value (for n samples) and z_i represents the measured in situ value. In equations (27)–(29), $\bar{x}$ and $\bar{z}$ are the average of the predicted and measured values, respectively. Furthermore, to statistically assess the significance of the results, the Student t test is applied. The estimated t value and the distribution at 0.05 significant level are used to calculate p values.

4. Results

4.1. Synthetic Experiment

The results of synthetic experiment, which is chosen to assess the capability of the two data assimilation schemes in improving model's simulation of physical processes, are presented in this section. TWS variations from W3RA (open loop; model integration without assimilation), AUKF, and Kalman-Takens filters (with $N = 14$ and $d = 11$; see section 4.2 for details), as well as synthetic observations, are displayed in Figure 2, where the time series represent spatially averaged TWS variations over the entire Iran. The trend lines corresponding to each time series are also depicted in the figure. As can be clearly seen, W3RA's open-loop run does not correctly capture the negative trend in the TWS time series as visible in the observations. Assimilation results, on the other hand, successfully reproduce the negative trend. Except for few cases, for example, 2009 and 2011, Kalman-Takens performs closely to AUKF. The assimilation trend lines also show that the filtered results capture the existing trend of the observations. In addition to the trends, there are larger correlations between AUKF (14% on average) and Kalman-Takens (12% on average) with the observations compared to the open-loop results. An evaluation of the assimilation results against the original WGHM TWS, that is, before perturbation using GRACE noises, are shown in Figure 3.

Figure 3 shows the scatterplot of the open-loop, AUKF, and Kalman-Takens TWS estimates against WGHM at the two spatial resolutions of $1^\circ \times 1^\circ$ and $3^\circ \times 3^\circ$ to assess the filters' performances at various spatial scales. Note that temporal assessment is also investigated in section 4.2. It can be seen that at both spatial scales,

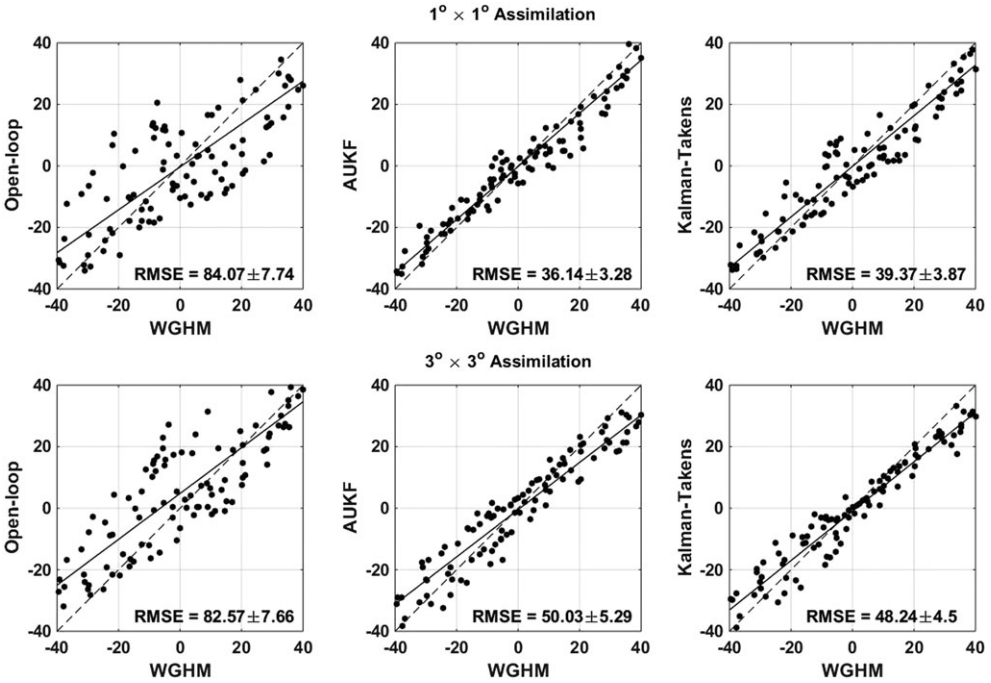

Figure 3. Scatterplots of open-loop, AUKF, and Kalman-Takens TWS estimates with respect to WGHM TWS at the two spatial resolution of 1° × 1° and 3° × 3°. The presented average RMSE values for each method is calculated based on the original WGHM TWS (before perturbation using GRACE errors). In each subfigure reference (dashed) and fitted (solid) lines are illustrated. AUKF = adaptive unscented Kalman filter; TWS = terrestrial water storage; WGHM = WaterGAP Global Hydrology Model; RMSE = root-mean-square error; GRACE = Gravity Recovery And Climate Experiment.

there are larger agreements between the filtered results and WGHM. There are also smaller RMSEs after filtering, which suggests the capability of both methods to improve model simulations even in case of remarkable human impact. While every assimilation scenario leads to smaller RMSE than the open-loop run, the least RMSEs are achieved at 1° × 1° resolution. This shows that assimilating TWS observations at a finer resolution can provide better estimates regardless of the filtering method. It can also be seen that both AUKF and Kalman-Takens provide comparable results at both spatial scales, leading to approximately 48% RMSE reduction. The filters' comparable results at 3° × 3° spatial resolution suggests their similar performance for downscaling TWS observations into the 1° × 1° W3RA resolution.

4.2. Assessment With In Situ Data

Independent groundwater and soil moisture in situ measurements within the Murray-Darling Basin in Australia are used to evaluate the results. This is done by comparing the AUKF and Kalman-Takens estimates of groundwater and soil moisture with those of the in situ measurements. Note that further analysis is undertaken to assess the impacts of the filters on nonassimilated variables and the results are provided in the supporting information. Before comparing AUKF and Kalman-Takens results against in situ measurements, we investigate the effect of various setups in the Kalman-Takens performance. Different scenarios are considered regarding the number of neighbors N (i.e., 2–40) and also the number of delays d (i.e., 1–25). To reach the best setup among these values, we compare the results of each scenario to the in situ groundwater measurements. Figure 4 shows the average absolute groundwater errors resulting from each case. Increasing the number of neighbors can improve the approximation of training data for a particular point to a certain extent (due to the existing spatial correlations). However, selecting N too large can cause a rapid growth of errors, which is related to the effect of oversmoothing the training step. This is different for delays d, where much larger errors are present for smaller values that underestimate temporal variabilities in the data. From our numerical investigations, it can be seen that applying the Kalman-Takens filter with $N = 14$ and $d = 11$ provides the best result. It is worth mentioning that we use these setups of the Kalman-Takens filter throughout this study.

The comparison between the open-loop run, AUKF, and Kalman-Takens results are depicted in Figure 5, which displays scatterplot of each filter's RMSE and STD calculated using in situ groundwater measurements.

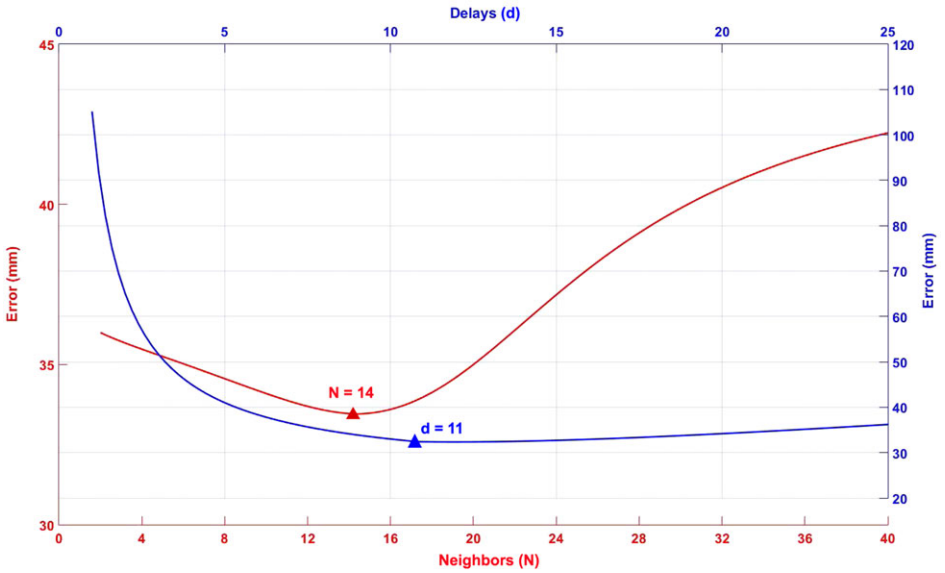

Figure 4. Estimated average errors from different scenarios considered based on the number of neighbors *N* and delays *d*. The best estimates are achieved by applying the Kalman-Takens method using $N = 14$ and $d = 11$.

Three different temporal evaluations are considered to further investigate the effect of temporal downscaling on the results. The GRACE TWS data (with approximately 30 days temporal scale) and associated errors are interpolated into a daily and 5-daily samples (see also Khaki, Schumacher, et al., 2017; Tangdamrongsub et al., 2015) using the spline interpolation between consecutive months. The assimilation is then undertaken on a daily, 5-day, and monthly basis. Figure 5 indicates that both AUKF and Kalman-Takens filters result in smaller RMSE and STD compared to the open-loop run for all the three temporal scales. In the daily and to a lesser degree 5-day assimilation cases, AUKF performs slightly better than the Kalman-Takens, with smaller RMSE and STD, which could be attributed to the contribution of the model equations for spreading TWS information between different variables after assimilation. Nevertheless, the performance of the nonparametric filter is satisfactory for both cases and comparable to that of AUKF. Interestingly, the performances of the two filters are even closer when assimilating monthly data. As a general result, this demonstrates that temporal downscaling of GRACE TWS data is recommended for data assimilation purpose regardless of the filtering method used. The average RMSE values for the 5-day assimilation using AUKF and Kalman-Takens filters are 51.28 (~13% smaller than daily and ~7% smaller than monthly) and 53.61 (~16% smaller than daily and ~5% smaller than monthly), respectively. Based on the above evaluation, it can be concluded that different

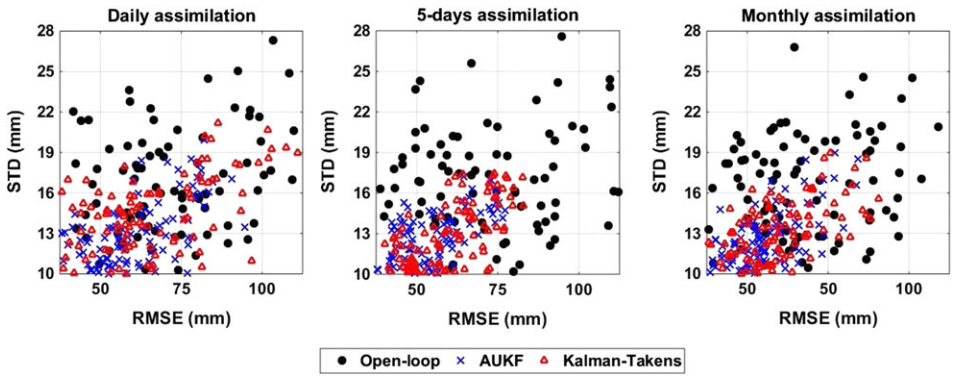

Figure 5. Average groundwater RMSE and STD of from the Kalman-Takens filter, AUKF, and open-loop run computed using groundwater in situ measurement. The results are presented for assimilation with three different temporal scales (i.e., daily, 5-day, and monthly). RMSE = root-mean-square error; STD = standard deviation; AUKF = adaptive unscented Kalman filter.

Table 1
Summary of Statistical Values Derived From the Implemented Methods Using the Groundwater In Situ Measurements

	Grid-based evaluation			Basin-scale evaluation		
Metric	Open loop	AUKF	Kalman-Takens	Open loop	AUKF	Kalman-Takens
RMSE (mm)	74.57	51.28	53.61	69.40	45.16	46.96
NSE	0.51	0.77	0.75	0.58	0.82	0.81
RMSE reduction (%)	—	31.23	28.11	—	34.93	32.33

Note. The reduction of the RMSE value of the AUKF and Kalman-Takens filters are calculated in relation to the RMSE of the open-loop run. AUKF = adaptive unscented Kalman filter; RMSE = root-mean-square error; NSE = Nash-Sutcliffe coefficient.

temporal scales have similar effects on both filters, where the AUKF and Kalman-Takens filters perform better for the 5-day assimilation case.

More detailed statistics are provided in Table 1 to better compare the performances of the implemented filters against in situ groundwater measurements. The evaluation is undertaken using RMSE and NSE metrics (see section 3.4) based on the 5-day assimilation case. Note that in this table, basin-scale results are provided in addition to the results of the grid-based evaluation. Considering the coarse spatial resolution of W3RA and the fact that a number of groundwater stations can be found in each grid cell, basin-averaged assessment is performed as an alternative examination. The spatially averaged open-loop results and those from filters over the Murray-Darling Basin are tested against basin-average groundwater time series. Results of Table 1 confirm the behavior seen in Figure 5. While smaller RMSEs are obtained from AUKF for both grid- and basin-based tests, the application of the Kalman-Takens method significantly decreases groundwater RMSE values (30.22% on average). Also, larger NSE values are obtained by both filters compared to the open-loop run. These results prove a high capability of the Kalman-Takens for improving state estimates, very close to the AUKF performance. Table 1 also indicates that the Kalman-Takens approach can be used as traditional data assimilation to reduce noise in the final state variables, which are the results of solving complex inverse problems; for example, groundwater estimates are improved from GRACE-derived TWS. This is also true for soil moisture estimates (cf. Table 2).

We use different soil moisture layers from in situ measurements including 0–8 (compared to the model top soil moisture layer), 0–30 (compared to the summation of the model top and shallow soil moisture layers), and 0–90 cm (compared to the summation of the model top, shallow, and deep soil moisture layers) for evaluating the results. Note that considering the difference between W3RA states (i.e., column water storage measured in mm) and the OzNet measurements (i.e., volumetric soil moisture) and the fact that converting the model outputs into volumetric units may introduce a bias (Renzullo et al., 2014), only NSE analysis is carried out and the results are provided in Table 2. Similar improvements as for groundwater evaluation are also found by comparing the filters estimates against OzNet soil moisture measurements (Table 2). Larger NSE values are found from data assimilation filters for all three soil layers. Average NSE from the Kalman-Takens method is 0.73, ~12.3% larger than the open-loop run, and slightly smaller than AUKF results (0.74). Table 2 confirms the capability of the Kalman-Takens method for improving the soil moisture estimates similar to AUKF

Table 2
Summary of NSE Values Estimated Using State Estimates Derived From Implemented Methods and the Soil Moisture In Situ Measurements at Different Layers

Method	0–8 cm	0–30 cm	0–90 cm
Open loop	0.59	0.64	0.72
AUKF	0.63	0.71	0.89
Kalman-Takens	0.61	0.73	0.85
Improvements (%)			
AUKF	6.77	10.94	23.61
Kalman-Takens	3.39	14.06	18.05

Note. The improvements (in %) are calculated based on the increased correlation by applying the methods with respect to the open-loop run. NSE = Nash-Sutcliffe coefficient; AUKF = adaptive unscented Kalman filter.

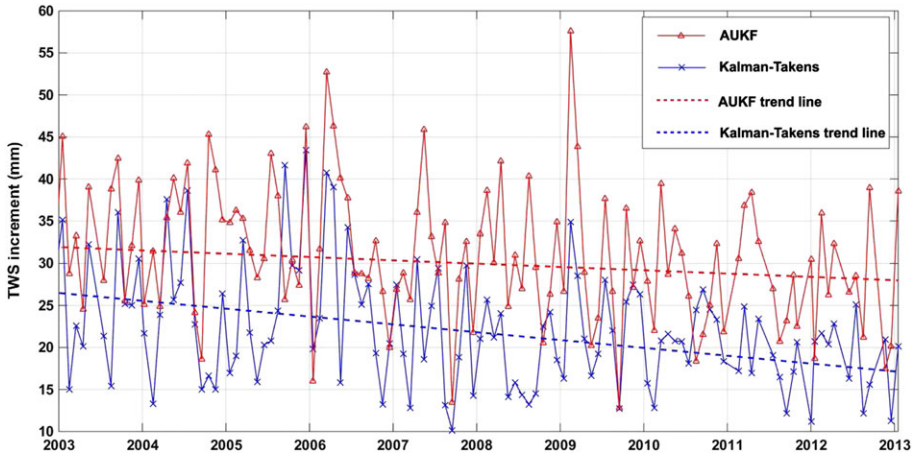

Figure 6. An average TWS increment time series of AUKF and the Kalman-Takens filter on state vectors during the process. Both methods decrease the increment as assimilation proceeds forward in time. TWS = terrestrial water storage; AUKF = adaptive unscented Kalman filter.

(13.7% on average). The largest improvements for both filters are achieved in the root zone (0–90 cm) moisture layer. Table 2 suggests that AUKF better reflects the GRACE observations, especially at this layer. This, however, does not necessarily lead to better approximations in the shallow soil moisture layer, where the nonparametric approach shows higher improvements compared to AUKF.

4.3. Assessing the Performance of AUKF and Kalman-Taken Filters

Here we compare the performances of the AUKF and Kalman-Takens filters from various perspectives including increment applied, state covariance, computational efficiency, and water storage forecasting. Figure 6 shows the increments implemented by each filtering technique during the study period. We estimate average increment (i.e., ϵ discussed in section 3.1) at all grid points for AUKF and the Kalman-Takens approach. One can see how the filters deal with the GRACE TWS observations in the update steps. Both methods decrease the increment as assimilation proceeds forward in time. This is found to be smaller for the Kalman-Takens method (see the trend lines in Figure 6) compared to AUKF. In fact, AUKF integrates the ensemble members through the model **f**, while the nonparametric approach uses the local proxy $\tilde{\mathbf{f}}$. Consequently, larger misfits between the Kalman-Takens method forecast estimates and observations can be expected. Nevertheless, Figure 6 shows that the local proxy performs comparably to **f** in most of the time. In addition to increments, the difference between the filter's forecasting also affects the estimated error covariances, especially forecast covariance matrix (cf. Figure 7).

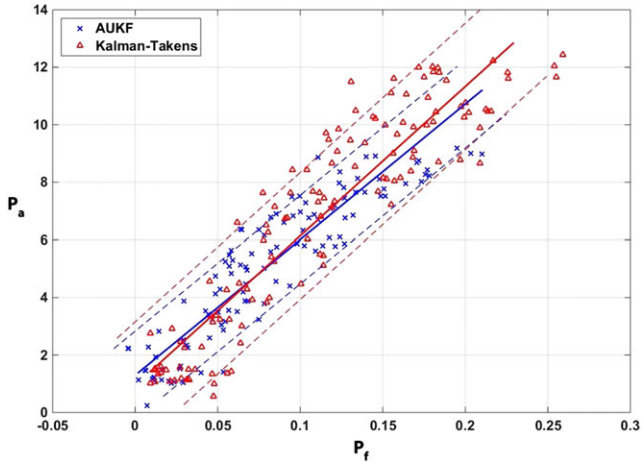

Figure 7. An average estimated covariance matrix of P_f and P_a corresponding to 95% confidence level (dashed lines) at each filtering step using the implemented filters. AUKF = adaptive unscented Kalman filter.

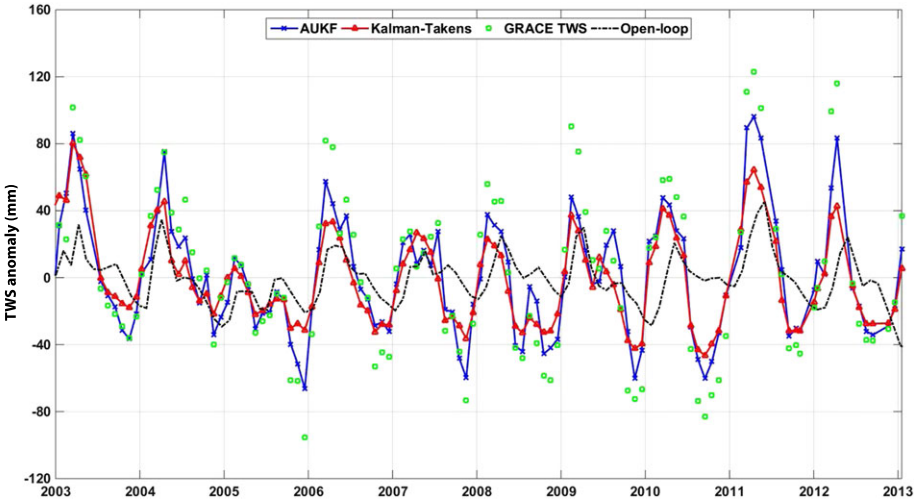

Figure 8. Spatially averaged TWS time series of filters' estimates, GRACE TWS observations, and open-loop run within Australia. TWS = terrestrial water storage; GRACE = Gravity Recovery And Climate Experiment; AUKF = adaptive unscented Kalman filter.

P_f and P_a are calculated at assimilation steps for both filters. The average of the matrices' diagonal elements are displayed in Figure 7. Despite the filters different performances in Figure 6, both methods perform very similar in dealing with the error covariances. The distribution of scattered error points from the Kalman-Takens filter and the corresponding trend line largely matches that of AUKF, which demonstrate that the filters have comparable uncertainty estimates. This indicates the ability of the Kalman-Takens method, which not only improves the model states but is also competitive with the traditional data assimilation system.

4.3.1. Filters Efficiency

Computational complexity is important for data assimilation methods, especially when dealing with a high-dimensional system, such as in hydrological studies. Therefore, a good data assimilation filter requires balancing between processes undertaken to achieve accurate estimates and computational efficiency. While the Kalman-Takens filter's capability for improving state estimates have already been demonstrated (cf. sections 4.1 and 4.2), its potential for decreasing the computational cost is examined here. This is done by comparing the computation time of the AUKF and Kalman-Takens filtering methods from various perspectives including forecasting, analysis steps, and filtering over the entire study period. Importantly, the following computation time estimates have been obtained using identical hardware. In the forecast step, the average computation time (for 794 grid points within Australia) is considerably lower for the Kalman-Takens filter, for example, 6.12 s against 8.57 s for AUKF. This is due to the fact that the Kalman-Takens filter exploits the proxy model ($\tilde{f}$), which is based on a local approximation and requires much less computation than a physics-based model. The average computational time at the analysis steps is 5.74 s for the Kalman-Takens filter and 7.83 s for AUKF. Considering that both methods are using similar analysis filtering, this difference is due to the local scheme (based on d delays and N neighbor points) in the Kalman-Takens method. The values of delays d and neighbors N determine the number of local points used in the analysis and accordingly the size of the underlying vectors and matrices. AUKF, on the other hand, solves for all grid points altogether, which requires a larger amount of memory and time. In general, it is found that the Kalman-Takens is considerably less computationally demanding, that is, $\sim$ 8 times faster for the entire experiment period, compared to the AUKF implementation for assimilating all observations into the system states.

4.3.2. Water Storage Update

In this section, we analyze the spatiotemporal increments derived by assimilating the GRACE TWS observations and explore their effects on the states. Figure 8 presents the average TWS time series after applying each filter, open-loop, and GRACE observations over Australia. Both filters largely decrease the misfits between the model states and the GRACE observations, which is expected since GRACE is used as a constraint. AUKF, however, has a larger impact on the states, especially where a significant TWS variation exists (e.g., 2006 and 2011–2012). The Kalman-Takens method, on the other hand, shows a smoother time series. Based on these results, we find that the Kalman-Takens approach is able to efficiently integrate observations into the model

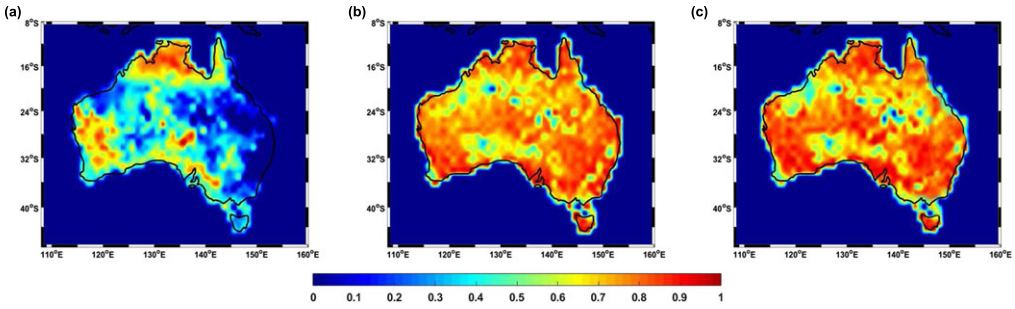

Figure 9. Spatial correlations maps between GRACE TWS and open-loop run (a), AUKF estimates (b), and the Kalman-Takens filter (c). GRACE = Gravity Recovery And Climate Experiment; TWS = terrestrial water storage; AUKF = adaptive unscented Kalman filter.

and correct missing trends as well as amplitudes and phases. Nevertheless, one can conclude that this method might not be able to efficiently extract spontaneous or high rate seasonal effects unless the training data have these variabilities/dynamics.

The correlation between the estimated TWS time series from the open-loop model run and the filters' estimates at each grid point within Australia and those of the GRACE TWS are presented in Figure 9. The filters largely increase the correlation between model derived TWS and those of GRACE. The largest correlations (with 0.92 average) is obtained by AUKF suggesting that this method better reflects the GRACE TWS into the states. The average correlation between TWS of the Kalman-Takens and GRACE is 0.89 (0.03 less than AUKF), and when compared to only 0.52 obtained from the open-loop estimates, the efficiency of the method becomes visible. Correlations of the open-loop TWS and GRACE are smaller over the mountainous area along the east coast compared to other parts of the country. This is due to difficulties of modeling hydrology in complex terrain areas (mountains). On the other hand, both assimilation methods show good performances by increased correlations with GRACE data. Over large parts of Australia, the performances of the Kalman-Takens filter and AUKF are found to be similar in terms of correlations with the GRACE TWS.

To further assess the capability of the filtering approaches for improving the model simulations, we test their ability in correcting the model variables for extreme and poorly known hydrological phenomena. To this end, the filters' TWS results are monitored between 2003 and 2012 over the Murray-Darling Basin. As shown by Schumacher et al. (2018), a long-term drought period (2001–2009), known as Millennium Drought (e.g., Le Blanc et al., 2012; Ummenhofer et al., 2009; van Dijk et al., 2013), has remarkably affected TWS variations in the basin. This negative TWS trend has then been followed by an above-average precipitation, mainly caused by El Niño Southern Oscillation (ENSO; see, e.g., Boening et al., 2012; Forootan et al., 2016) for the period of 2010–2012. Here we investigate the capability of the open-loop, AUKF, and Kalman-Takens TWS estimates to capture these two extreme events. Figure 10 plots the average TWS time series of the above methods, as well as GRACE-derived TWS over the Murray-Darling Basin. As can be seen, while both Millennium drought (red shaded area) and ENSO effect (blue shaded area) are reflected in GRACE TWS time series,

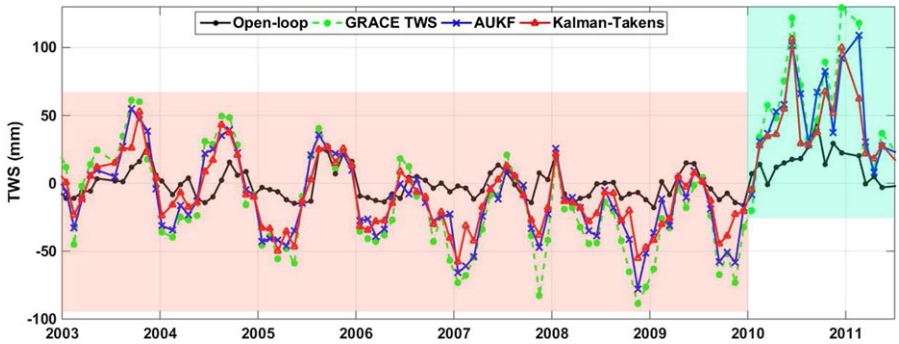

Figure 10. Average TWS variations from the data assimilation filters, open-loop run, and GRACE TWS. The red shaded area shows the Millennium Drought, and blue shaded area represents a strong ENSO effect. GRACE = Gravity Recovery And Climate Experiment; TWS = terrestrial water storage; ENSO = El Niño Southern Oscillation.

the open-loop run is unable to capture them, especially the drought effects. AUKF and the Kalman-Takens filter, on the other hand, successfully depict the negative trend between 2003 and 2010, followed by a positive anomaly after 2010. Except for few points such as 2004, 2007, and late 2009, the Kalman-Takens method presents a similar performance as AUKF in incorporating GRACE TWS data with states and reflecting extreme hydrological events.

5. Conclusions

The present study investigates the ability of the Kalman-Takens approach to reconstruct the nonlinear dynamics of a hydrological model. This is done to update observable state variables based on new observations when a physics-based model is not available. This implies that contrary to a standard data assimilation, the Kalman-Takens filter does not affect nonobserved variables (e.g., water discharge in our case). In this work, we introduce a new setup for the Kalman-Takens filter to reconstruct additional states (e.g., soil moisture and groundwater) using the GRACE TWS. The Kalman-Takens results are compared with a parametric forecasting approach of an AUKF as well as against in situ groundwater and soil moisture measurements. The results prove a high capability of the Kalman-Takens for improving state estimates, largely comparable to the AUKF performance, and as such, both provide efficient methods for assimilating GRACE TWS data. Results indicate that smaller RMSE (46.96 mm) and higher NSE (0.82) values are obtained from the application of the Kalman-Takens method in comparison to the open-loop run (69.40 mm RMSE and 0.58 NSE). Although AUKF performs slightly better in some cases, for example, ∼3% higher improvement for groundwater estimates, which is expected since AUKF takes advantage of the full knowledge of the model while the nonparametric filter uses only the short noisy training data set from which to learn the dynamics, in all cases considered, the Kalman-Takens results are generally very close to those of AUKF. The data-driven approach also increases the NSE values between the estimated soil moisture variations and the OzNet in situ measurements for all soil layers (11.83% on average) as compared to AUKF (13.77% on average). The proposed approach also reduces estimation complexities by using the local proxy model. The Kalman-Takens filter performs more efficient (∼8 times faster) in terms of computational cost, which is very important to deal with a growing amount of data sets in high-dimensional systems. This contribution, to the best of the authors' knowledge, is the first effort in using the data-driven approach in hydrological studies with complex state observation transition systems. Further research should be undertaken to investigate the Kalman-Takens filter in different hydrological applications and also to explore its capability in dealing with multiple satellite products.

Acknowledgments

We would like to thank Tyrus Berry and Timothy Sauer for their valuable help in this study. M. Khaki is grateful for the research grant of Curtin International Postgraduate Research Scholarships (CIPRS)/ORD Scholarship provided by Curtin University (Australia). F. Hamilton is supported by National Science Foundation grant RTG/DMS-1246991. This work is a TIGeR publication. The GRACE data are acquired from the ITSG-Grace2014 gravity field model (Mayer-Gürr et al., 2014). In situ groundwater and soil moisture measurements are obtained from the New South Wales Government (NSW; http://waterinfo.nsw.gov.au/pinneena/gw.shtml) and the OzNet network (http://www.oznet.org.au/), respectively. Meteorological forcing data are provided by Princeton University (http://hydrology.princeton.edu). Other data used in this study can be found at DOI: 10.6084/m9.figshare.5942548. A more detailed discussion of the results can be found in the supporting information (Huffman et al., 2007; Mu et al., 2011).

References

Andreadis, K. M., Clark, E. A., Lettenmaier, D. P., & Alsdorf, D. E. (2007). Prospects for river discharge and depth estimation through assimilation of swath-altimetry into a raster-based hydrodynamics model. *Geophysical Research Letters*, *34*, L11607. https://doi.org/10.1029/2007GL02972

Arnold, H., Moroz, I., & Palmer, T. (2013). Stochastic parametrizations and model uncertainty in the Lorenz '96 System. *Philosophical Transactions of the Royal Society A*, *371*, 20110479.

Awwad, H. M., Valdés, J. B., & Restrepo, P. J. (1994). Streamflow forecasting for Han River basin, Korea. *Journal of Water Resources Planning and Management*, *120*, 651–673.

Bennett, A. F. (2002). *Inverse modeling of the ocean and atmosphere*. (p. 234). New York: Cambridge University Press.

Berry, T., & Harlim, J. (2016). Variable bandwidth diffusion kernels. *Applied and Computational Harmonic Analysis*, *40*, 68–96.

Berry, T., & Sauer, T. (2013). Adaptive ensemble Kalman filtering of non-linear systems. *Tellus A: Dynamic Meteorology and Oceanography*, *65*(1), 20331. https://doi.org/10.3402/tellusa.v65i0.20331

Boening, C., Willis, J. K., Landerer, F. W., Nerem, R. S., & Fasullo, J. (2012). The 2011 La Niña: So strong, the oceans fell. *Geophysical Research Letters*, *39*, L19602. https://doi.org/10.1029/2012GL053055

Bras, R. L., & Restrepo-Posada, P. (1980). Real time automatic parameter calibration in conceptual runoff forecasting models. In *Proceedings of the 3rd international symposium on Stochastic Hydraulics*, Tokyo, pp. 61–70.

Brocca, L., Melone, F., Moramarco, T., Wagner, W., Naeimi, V., Bartalis, Z., & Hasenauer, S. (2010). Improving runoff prediction through the assimilation of the ASCAT soil moisture product. *Hydrology and Earth System Sciences*, *14*, 1881–1893. https://doi.org/10.5194/hess-14-1881-2010

Calvet, J.-C., Noilhan, J., & Bessemoulin, P. (1998). Retrieving root-zone soil moisture from surface soil moisture of temperature estimates: A feasibility study based on field measurements. *Journal of Applied Meteorology*, *37*, 371–386.

Cheng, M. K., & Tapley, B. D. (2004). Variations in the Earth's oblateness during the past 28 years. *Journal of Geophysical Research*, *109*, B09402. https://doi.org/10.1029/2004JB003028

Chiew, F. H. S., Stewardson, M. J., & McMahon, T. A. (1993). Comparison of six rainfall-runoff modelling approaches. *Journal of Hydrology*, *147*, 1–36.

Christiansen, L., Krogh, P. E., Bauer-Gottwein, P., Andersen, O. B., Leirião, S., Binning, P. J., & Rosbjerg, D. (2007). Local to regional hydrological model calibration for the Okavango River basin from in-situ and space borne gravity observations, Proceedings of 2nd Space for Hydrology Workshop, pp. 12–14.

Coumou, D., & Rahmstorf, S. (2012). A decade of weather extremes. *Nature Climate Change*, *2*(7), 1–6.

De Lannoy, G. J. M, de Rosnay, P., & Reichle, R. H. (2015). Soil moisture data assimilation. In Q. Duan, et al. (Eds.), *Handbook of hydrometeorological ensemble forecasting*. Berlin, Heidelberg: Springer.

De Lannoy, G. J. M., Houser, P. R., Pauwels, V. R. N., & Verhoest, N. E. (2009). Assessment of model uncertainty for soil moisture through ensemble verification. *Journal of Geophysical Research*, *111*, D10101. https://doi.org/10.1029/2005JD006367

De Lannoy, G., Pauwels, V. R. N., Houser, P. R., Verhoest, N. E. C., & Gish, T. (2007). Representativeness of point soil moisture observations, upscaling and assimilation. In *IUGG General Assembly*, Perugia Italy. Session HS2004.

De Lannoy, G. J. M., Reichle, R. H., Houser, P. R., Pauwels, V. R. N., & Verhoes, N. E. C. (2007). Correcting for forecast bias in soil moisture assimilation with the ensemble Kalman filter. *Water Resources Research*, *43*, W09410. https://doi.org/10.1029/2006WR00544

Döll, P., Kaspar, F., & Lehner, B. (2003). A global hydrological model for deriving water availability indicators: Model tuning and validation. *Journal of Hydrology*, *270*, 105–134.

Dreano, D., Mallick, B., & Hoteit, I. (2015). Filtering remotely sensed chlorophyll concentrations in the Red Sea using a space–time covariance model and a Kalman filter. *Spatial Statistics*, *13*, 1–20. https://doi.org/10.1016/j.spasta.2015.04.002

Eicker, A., Schumacher, M., Kusche, J., Döll, P., & Müller-Schmied, H. (2014). Calibration/data assimilation approach for integrating GRACE data into the WaterGAP global hydrology model (WGHM) using an ensemble Kalman filter: First results. *Surveys in Geophysics*, *35*(6), 1285–1309. https://doi.org/10.1007/s10712-014-9309-8

Entekhabi, D., Nakamura, H., & Njoku, E. G. (1994). Solving the inverse problem for soil moisture and temperature profiles by sequential assimilation of multifrequency remotely senses observations. *IEEE Transactions on Geoscience and Remote Sensing*, *32*, 438–448.

Famiglietti, J. S., Ryu, D., Berg, A. A., Rodell, M., & Jackson, T. J. (2008). Field observations of soil moisture variability across scales. *Water Resources Research*, *44*, W01423. https://doi.org/10.1029/2006WR005804

Forootan, E., Khandu, Awange, Schumacher, M., Anyah, R., van Dijk, A., & Kusche, J. (2016). Quantifying the impacts of ENSO and IOD on rain gauge and remotely sensed precipitation products over Australia. *Remote Sensing of Environment*, *172*, 50–66. https://doi.org/10.1016/j.rse.2015.10.027

Forootan, E., Safari, A., Mostafaie, A., Schumacher, M., Delavar, M., & Awange, J. (2017). Large-scale total water storage and water flux changes over the arid and semiarid parts of the middle east from grace and reanalysis products. *Surveys in Geophysics*, *38*(3), 591–615. https://doi.org/10.1007/s10712-016-9403-1

Girotto, M., De Lannoy, G. J. M, Reichle, R. H., & Rodell, M. (2016). Assimilation of gridded terrestrial water storage observations from GRACE into a land surface model. *Water Resources Research*, *52*, 4164–4183. https://doi.org/10.1002/2015WR018417

Girotto, M., De Lannoy, G. J. M., Reichle, R. H., Rodell, M., Draper, C., Bhanja, S. N., & Mukherjee, A. (2017). Benefits and pitfalls of GRACE data assimilation: A case study of terrestrial water storage depletion in India. *Geophysical Research Letters*, *44*, 4107–4115. https://doi.org/10.1002/2017GL072994

Giustarini, L., Matgen, P., Hostache, R., Montanari, M., Plaza, D., Pauwels, V. R. N., et al. (2011). Assimilating SAR-derived water level data into a hydraulic model: A case study. *Hydrology and Earth System Sciences*, *15*, 2349–2365. https://doi.org/10.5194/hess-15-2349-2011

Hamilton, F., Berry, T., & Sauer, T. (2015). Predicting chaotic time series with a partial model. *Physical Review E*, *92*, 010902.

Hamilton, F., Berry, T., & Sauer, T. (2016). Ensemble Kalman filtering without a model. *Physical Review X6*, *6*, 011021. https://doi.org/10.1103/PhysRevX.6.011021

Hamilton, F., Berry, T., & Sauer, T. (2017). Kalman-Takens filtering in the presence of dynamical noise. *European Physical Journal - Special Topics*, *226*(15), 3239–3250.

Hersbach, H., Stoffelen, A., & De Haan, S. (2007). An improved C-band scatterometer ocean geophysical model function: CMOD5. *Journal of Geophysical Research*, *112*, C03006. https://doi.org/10.1029/2006JC003743

Hoteit, I., Luo, X., & Pham, D. T. (2012). Particle Kalman filtering: A nonlinear Bayesian framework for ensemble Kalman filters. *Monthly Weather Review*, *140*(2), 528–542.

Hoteit, I., Pham, D. T., & Blum, J. (2002). A simplified reduced-order kalman filtering and application to altimetric data assimilation in tropical Pacific. *Journal of Marine Systems*, *36*, 101–127.

Huang, S., Kumar, R., Flörke, M., Yang, T., Hundecha, Y., Kraft, P., et al. (2016). Evaluation of an ensemble of regional hydrological models in 12 large-scale river basins worldwide. *Climate Change*, *141*(3), 381–397. https://doi.org/10.1007/s10584-016-1841-8

Huffman, G. J., Adler, R. F., Bolvin, D. T., Gu, G., Nelkin, E. J., Bowman, K. P., et al. (2007). The TRMM multi-satellite precipitation analysis: Quasi-global, multi-year, combined-sensor precipitation estimates at fine scale. *Journal of Hydrometeorology*, *8*(1), 38–55.

Huntington, T. G. (2006). Evidence for intensification of the global water cycle: Review and synthesis. *Journal of Hydrology*, *319*(1–4), 83–95. https://doi.org/10.1016/j.jhydrol.2005.07.003

Irmak, A., & Kamble, B. (2009). Evapotranspiration data assimilation with genetic algorithms and SWAP model for on-demand irrigation. *Irrigation Science*, *28*(1), 101–112.

Jian, Y., Chesheng, Z., Hongliang, G., & Feiyu, W. (2014). A case study of evapotranspiration data assimilation based bon hydrological model. *Advances in Earth Science*, *29*(9), 1075–1084.

Julier, S. J., & Uhlmann, J. K. (1997). A new extension of the Kalman filter to nonlinear systems. In *Proceeding of AeroSense: The 11th International Symposium on Aerospace/Defence Sensing, Simulation and Controls*, Orlando, FL, USA.

Julier, S. J., & Uhlmann, J. K. (2004). Unscented filtering and nonlinear estimation. *Proceedings of the IEEE*, *92*, 401–422.

Julier, S., Uhlmann, J., & Durrant-Whyte, H. F. (2000). A new method for the nonlinear transformation of means and covariances in filters and estimators. *IEEE Transactions on Automatic Control*, *45*, 477–482.

Kalnay, E. (2003). *Atmospheric modelling, data assimilation and predictability* (pp. xxii 341.). Cambridge, UK: Cambridge University Press. https://doi.org/10.1256/003590003606835111

Khaki, M., Ait-El-Fquih, B., Hoteit, I., Forootan, E., Awange, J., & Kuhn, M. (2017). A two-update ensemble Kalman filter for land hydrological data assimilation with an uncertain constraint. *Journal of Hydrology*, *555*, 447–462. https://doi.org/10.1016/j.jhydrol.2017.10.032

Khaki, M., Forootan, E., Kuhn, M., Awange, J., Longuevergne, L., & Wada, W. (2018). Efficient basin scale filtering of GRACE satellite products. *Remote Sensing of Environment*, *204*, 76–93. https://doi.org/10.1016/j.advwatres.2018.02.008

Khaki, M., Forootan, E., Kuhn, M., Awange, J., Papa, F., & Shum, C. K. (2018). A study of Bangladesh's sub-surface water storages using satellite products and data assimilation scheme. *Advances in Water Resources*, *625*, 963–977.

Khaki, M., Forootan, E., Kuhn, M., Awange, J., van Dijk, A. I. J. M., Schumacher, M., & Sharifi, M. A. (2018). Determining water storage depletion within Iran by assimilating GRACE data into the W3RA hydrological model. *Advances in Water Resources*, *114*, 1–18.

Khaki, M., Hoteit, I., Kuhn, M., Awange, J., Forootan, E., van Dijk, A. I. J. M., et al. (2017). Assessing sequential data assimilation techniques for integrating GRACE data into a hydrological model. *Advances in Water Resources*, *107*, 301–316. https://doi.org/10.1016/j.advwatres.2017.07.001

Khaki, M., Schumacher, M., Forootan, E., Kuhn, M., Awange, J. L., & van Dijk, A. I. J. M. (2017). Accounting for spatial correlation errors in the assimilation of GRACE into hydrological models through localization. *Advances in Water Resources*, *108*, 99–112. https://doi.org/10.1016/j.advwatres.2017.07.024

Kumar, S. V., Peters-Lidard, C. D., Santanello, J. A., Reichle, R. H., Draper, C. S., Koster, R. D., et al. (2015). Evaluating the utility of satellite soil moisture retrievals over irrigated areas and the ability of land data assimilation methods to correct for unmodeled processes. *Hydrology and Earth System Sciences*, *19*, 4463–4478. https://doi.org/10.5194/hess-19-4463-2015

Kumar, S. V., Reichle, R. H., Koster, R. D., Crow, W. T., & Peters-Lidard, C. D. (2009). Role of subsurface physics in the assimilation of surface soil moisture observations. *Journal of Hydrometeorology*, *10*(6), 1534–1547. https://doi.org/10.1175/2009JHM1134.1

Kumar, S., Zaitchik, B., Peters-Lidard, C., Rodell, M., Reichle, R., Li, B., et al. (2016). Assimilation of gridded GRACE terrestrial water storage estimates in the North American land data assimilation system. *Journal of Hydrometeorology*, *17*, 1951–1972. https://doi.org/10.1175/JHM-D-15-0157.1

Kusche, J., Schmidt R., Petrovic, S., & Rietbroek, R. (2009). Decorrelated GRACE time-variable gravity solutions by GFZ and their validation using a hydrological model. *Journal of Geodesy*, *83*(10), 903–913. https://doi.org/10.1007/s00190-009-0308-3

Lagergren, J., Reeder, A., Hamilton, F., Smith, R. C., & Flores, K. B. (2018). Forecasting and uncertainty quantification using a hybrid of mechanistic and non-mechanistic models for an age-structured population model. *Bulletin of Mathematical Biology*, *80*(6), 1578–1595. https://doi.org/10.1007/s11538-018-0421-7

Lahoz, W. A., Geer, A. J., Bekki, S., Bormann, N., Ceccherini, S., Elbern, H., et al. (2007). The Assimilation of Envisat data (ASSET) project. *Atmospheric Chemistry and Physics*, *7*, 1773–1796.

Le Blanc, M., Tweed, S., Van Dijk, A., & Timbal, B. (2012). A review of historic and future hydrological changes in the Murray Darling Basin. *Global Planetary Change*, *80–81*, 226–246.

Lee, H., Seo, D.-J., & Koren, V. (2011). Assimilation of streamflow and in situ soil moisture data into operational distributed hydrologic models: Effects of uncertainties in the data and initial model soil moisture states. *Advances in Water Resources*, *34*(12), 1597–1615. https://doi.org/10.1016/j.advwatres.2011.08.012

Lguensat, R., Tandeo, P., Ailliot, P., Pulido, M., & Fablet, R. (2017). The analog data assimilation. *Monthly Weather Review*, *145*, 4093–4107. https://doi.org/10.1175/MWR-D-16-0441.1

Li, Y., Ryu, D., Western, A. W., & Wang, Q. J. (2015). Assimilation of stream discharge for flood forecasting: Updating a semidistributed model with an integrated data assimilation scheme. *Water Resources Research*, *51*, 3238–3258. https://doi.org/10.1002/2014WR016667

Lievens, H., Kumar, S., Al Bitar, A., De Lannoy, G. J. M., Drusch, M., Dumedah, G., et al. (2015). SMOS soil moisture assimilation for improved hydrologic simulation in the Murray Darling Basin, Australia. *Remote Sensing of Environment*, *168*(10), 146–162.

Madsen, H., & Skotner, C. (2005). Adaptive state-updating in real-time river flow forecasting–A combined filtering and error forecasting procedure. *Journal of Hydrology*, *308*, 302–312.

Mayer-Gürr, T., Zehentner, N., Klinger, B., & Kvas, A. (2014). ITSG-Grace2014: A new GRACE gravity field release computed in Graz. In *GRACE Science Team Meeting (GSTM)*, Potsdam.

McMillan, H. K., Hreinsson, E. Ã., Clark, M. P., Singh, S. K., Zammit, C., & Uddstrom, M. J. (2013). Operational hydrological data assimilation with the recursive ensemble Kalman filter. *Hydrology and Earth System Sciences*, *17*(1), 21–38. https://doi.org/10.5194/hess-17-21-2013

Mehra, R. (1970). On the identification of variances and adaptive Kalman filtering. *IEEE Transactions on Automatic Control*, *15*, 175–184.

Mehra, R. (1972). Approaches to adaptive filtering. *IEEE Transactions on Automatic Control*, *17*, 693–698.

Mercer, D., Christesen, L., & Buston, M. (2007). Squandering the future—Climate change, policy failure and the water crisis in Australia. *Futures*, *39*, 272–287.

Montaldo, N., Albertson, J. D., Mancini, M., & Kiely, G. (2001). Robust simulation of root zone soil moisture with assimilation of surface soil moisture data. *Water Resources Research*, *37*, 2889–2900.

Mu, Q., Zhao, M., & Running, S. W. (2011). Improvements to a MODIS global terrestrial evapotranspiration algorithm. *Remote Sensing of Environment*, *115*, 1781–1800.

Müller Schmied, H., Eisner, S., Franz, D., Wattenbach, M., Portmann, F., Flörke, M., & Döll, P. (2014). Sensitivity of simulated global-scale freshwater fluxes and storages to input data, hydrological model structure, human water use and calibration. *Hydrology and Earth System Sciences*, *18*, 3511–3538. https://doi.org/10.5194/hess-18-3511-2014

Neal, J., Schumann, G., Bates, P., Buytaert, W., Matgen, P., & Pappenberger, F. (2009). A data assimilation approach to discharge estimation from space. *Hydrological Processes*, *23*, 3641–3649.

Nicolai-Shaw, N., Hirschi, M., Mittelbach, H., & Seneviratne, S. I. (2015). Spatial representativeness of soil moisture using in situ, remote sensing, and land reanalysis data. *Journal of Geophysical Research: Atmospheres*, *120*, 9955–9964. https://doi.org/10.1002/2015JD023305

Orlowsky, B., & Seneviratne, S. I. (2014). On the spatial representativeness of temporal dynamics at European weather stations. *International Journal of Climatology*, *34*(10), 3154–3160. https://doi.org/10.1002/joc.3903

Packard, N. H., Crutchfield, J. P., Farmer, J. D., & Shaw, R. S. (1980). Geometry from a time series. *Physical Review Letters*, *45*, 712.

Palmer, T. N. (2001). A nonlinear dynamical perspective on model error: A proposal for non-local stochastic-dynamic parametrization in weather and climate prediction models. *Quarterly Journal of the Royal Meteorological Society*, *127*, 279–304.

Pipunic, C., Walker, P., & Western, A. (2008). Assimilation of remotely sensed data for improved latent and sensible heat flux prediction: A comparative synthetic study. *Remote Sensing of Environment*, *112*(4), 1295–1305.

Rasmussen, J., Madsen, H., Jensen, K. H., & Refsgaard, J. C. (2015). Data assimilation in integrated hydrological modeling using ensemble Kalman filtering: Evaluating the effect of ensemble size and localization on filter performance. *Hydrology and Earth System Sciences*, *19*, 2999–3013. https://doi.org/10.5194/hess-19-2999-2015

Reager, J. T., Thomas, A. C., Sproles, E. A., Rodell, M., Beaudoing, H. K., Li, B., & Famiglietti, J. S. (2015). Assimilation of grace terrestrial water storage observations into a land surface model for the assessment of regional flood potential. *Remote Sensing of Environment*, *2015*(7), 14663–14679.

Reichle, R. H., & Koster, R. D. (2005). Global assimilation of satellite surface soil moisture retrievals into the NASA catchment land surface model. *Geophysical Research Letters*, *32*, L02404. https://doi.org/10.1029/2004GL021700

Reichle, R. H., McLaughlin, D. B., & Entekhabi, D. (2002). Hydrologic data assimilation with the ensemble Kalman filter. *Monthly Weather Review*, *130*, 103–114. https://doi.org/10.1175/1520-0493(2002)130<0103:HDAWTE>2.0.CO;2

Renzullo, L. J., van Dijk, A. I. J. M., Perraud, J. M., Collins, D., Henderson, B., Jin, H., et al. (2014). Continental satellite soil moisture data assimilation improves root-zone moisture analysis for water resources assessment. *Journal of Hydrology*, *519*, 2747–2762. https://doi.org/10.1016/j.jhydrol.2014.08.008

Rodell, M., Chen, J., Kato, H., Famiglietti, J. S., Nigro, J., & Wilson, C. R. (2007). Estimating groundwater storage changes in the Mississippi River basin (USA) using GRACE. *Hydrogeology Journal*, *15*, 159–166.

Sauer, T. (2004). Reconstruction of shared nonlinear dynamics in a network. *Physical Review Letters*, *93*, 198701.

Sauer, T., Yorke, J., & Casdagli, M. (1991). Embedology. *Journal of Statistical Physics*, *65*, 579–616.
Schumacher, M., Forootan, E., van Dijk, A. I. J. M., Müller Schmied, H., Crosbie, R. S., Kusche, J., & Döll, P. (2018). Improving drought simulations within the Murray-Darling Basin by combined calibration/assimilation of GRACE data into the WaterGAP Global Hydrology Model. *Remote Sensing of Environment*, *204*, 212–228. https://doi.org/10.1016/j.rse.2017.10.029
Schumacher, M., Kusche, J., & Döll, P. (2016). A systematic impact assessment of GRACE error correlation on data assimilation in hydrological models. *Journal of Geodesy*, *90*(6), 537–559. https://doi.org/10.1007/s00190-016-0892-y
Schunk, R. W., Scherliess, L., Sojka, J. J., & Thompson, D. C. (2004). USU global ionospheric data assimilation models, atmospheric and environmental remote sensing data processing and utilization: An end-to-end system perspective. In H.-L. A. Huang & H. J. Bloom (Eds.), *Proceedings of SPIE* (Vol. 5548, pp. 327–336). https://doi.org/10.1117/12.562448
Schuurmans, M., Troch, A., Veldhuizen, A., & et al. (2003). Assimilation of remotely sensed latent heat flux in a distributed hydrological model. *Advances in Water Resources*, *26*(2), 151–159.
Seo, D. J., Koren, V., & Cajina, N. (2003). Real-time variational assimilation of hydrologic and hydrometeorological data into operational hydrologic forecasting. *Journal of Hydrometeorology*, *4*, 627–641.
Seoane, L., Ramillien, G., Frappart, F., & Leblanc, M. (2013). Regional GRACE-based estimates of water mass variations over Australia: Validation and interpretation. *Hydrology and Earth System Sciences*, *17*, 4925–4939. https://doi.org/10.5194/hess-17-4925-2013
Sheffield, J., Goteti, G., & Wood, E. F. (2006). Development of a 50-year high-resolution global dataset of meteorological forcings for land surface modeling. *Journal of Climate*, *19*(13), 3088–3111.
Simon, D. (2006). *Optimal state estimation: Kalman, H_∞, and nonlinear approaches*. New York, NY: John Wiley and Sons.
Smith, P. J., Dance, S. L., & Nichols, N. K. (2011). A hybrid data assimilation scheme for model parameter estimation: Application to morphodynamic modelling. *Computers and Fluids*, *46*(1), 436–441. https://doi.org/10.1016/j.compfluid.2011.01.010
Song, Q., & He, Y. (2009). Adaptive unscented Kalman filter for estimation of modelling errors for helicopter, IEEE International Conference on Robotics and Biomimetics (ROBIO). *Guilin*, *2009*, 2463–2467. https://doi.org/10.1109/ROBIO.2009.5420406
Swenson, S., Chambers, D., & Wahr, J. (2008). Estimating geocentervariations from a combination of GRACE and ocean model output. *Journal of Geophysical Research*, *113*, B08410. https://doi.org/10.1029/2007JB005338
Takens, F. (1981). *Dynamical systems and turbulence, Warwick 1980* (Vol. 898, pp. 366), Lecture notes in mathematics. Berlin Heidelberg: Springer-Verlag.
Tandeo, P., Ailliot, P., Ruiz, J., Hannart, A., Chapron, B., Cuzol, A., et al. (2015). Combining analog method and ensemble data assimilation: Application to the Lorenz-63 chaotic system, *Machine learning and data mining approaches to climate science* (pp. 3–12). Switzerland: Springer.
Tangdamrongsub, N., Steele-Dunne, S. C., Gunter, B. C., Ditmar, P. G., & Weerts, A. H. (2015). Data assimilation of GRACE terrestrial water storage estimates into a regional hydrological model of the Rhine River basin. *Hydrology and Earth System Sciences*, *19*, 2079–2100. https://doi.org/10.5194/hess-19-2079-2015
Tardif, R., Hakim, G. J., & Snyder, C. (2015). Coupled atmosphere–ocean data assimilation experiments with a low-order model and CMIP5 model data. *Climate Dynamics*, *45*, 1415. https://doi.org/10.1007/s00382-014-2390-3
Terejanu, G. A. (2009). Unscented Kalman filter tutorial, Workshop on large-scale quantification of uncertainty. *Sandia National Laboratories*, 1–6.
Tian, S., Tregoning, P., Renzullo, L. J., van Dijk, A. I. J. M., Walker, J. P., Pauwels, V. R. N., & Allgeyer, S. (2017). Improved water balance component estimates through joint assimilation of GRACE water storage and SMOS soil moisture retrievals. *Water Resources Research*, *53*, 1820–1840. https://doi.org/10.1002/2016WR019641
Ummenhofer, C. C., England, M. H., McIntosh, P. C., Meyers, G. A., Pook, M. J., Risbey, J. S., et al. (2009). What causes southeast Australia's worst droughts*Geophysical Research Letters*, *36*, L04706. https://doi.org/10.1029/2008GL036801
van Dijk, A. I. J. M. (2010). The Australian water resources assessment system: Technical report 3, *Landscape model (version 0.5) technical description*.
van Dijk, A. I. J. M., Peña-Arancibia, J. L., Wood, E. F., Sheffield, J., & Beck, H. E. (2013). Global analysis of seasonal streamflow predictability using an ensemble prediction system and observations from 6192 small catchments worldwide. *Water Resources Research*, *49*, 2729–2746. https://doi.org/10.1002/wrcr.20251
van Dijk, A. I. J. M., Renzullo, L. J., & Rodell, M. (2011). Use of Gravity Recovery And Climate Experiment terrestrial water storage retrievals to evaluate model estimates by the Australian water resources assessment system. *Water Resources Research*, *47*, W11524. https://doi.org/10.1029/2011WR010714
van Dijk, A. I. J. M., Renzullo, L. J., Wada, Y., & Tregoning, P. (2014). A global water cycle reanalysis (2003–2012) merging satellite gravimetry and altimetry observations with a hydrological multi-model ensemble. *Hydrology and Earth System Sciences*, *18*, 2955–2973. https://doi.org/10.5194/hess-18-2955-2014
Van der Merwe, R. (2004). Sigma-point Kalman filters for probability inference in dynamic state-space models (PhD thesis), Oregon Health and Science University.
Vrugt, J. A., Diks, C. G., Gupta, H. V., Bouten, W., & Verstraten, J. M. (2005). Improved treatment of uncertainty in hydrologic modeling: Combining the strengths of global optimization and data assimilation. *Water Resources Research*, *41*, W01017. https://doi.org/10.1029/2004WR003059
Vrugt, J. A., Gupta, H. V., & Nuallain, B. O. (2006). Real-time data assimilation for operational ensemble streamflow forecasting. *Journal of Hydrometeorology*, *7*(3), 548–565. https://doi.org/10.1175/JHM504.1
Vrugt, J. A., ter Braak, C. J. F., Diks, C. G. H., & Schoups, G. (2013). Advancing hydrologic data assimilation using particle Markov chain Monte Carlo simulation: Theory, concepts and applications. *Advances in Water Resources Anniversary Issue—35 Years*, *51*, 457–478. https://doi.org/10.1016/j.advwatres.2012.04.002
Wahr, J. M., Molenaar, M., & Bryan, F. (1998). Time variability of the Earth's gravity field: Hydrological and oceanic effects and their possible detection using GRACE. *Journal of Geophysical Research*, *108*(B12), 30,205–30,229. https://doi.org/10.1029/98JB02844
Wan, E., & van der Merwe, R. (2000). The unscented Kalman filter for nonlinear estimation, *Proceedings of the IEEE 2000 Adaptive Systems for Signal Processing, Communications, and Control Symposium (Cat. No.00EX373)* (Vol. 2000, pp. 153–158). Lake Louise, Alta.https://doi.org/10.1109/ASSPCC.2000.882463
Wan, E., & van der Merwe, R. (2001). The unscented Kalman filter. In S. Haykin (Ed.), *Kalman Filtering and Neural Networks* (Chap. 7, pp. 221–280). New York: Wiley.
Weerts, A. H., & El Serafy, G. Y. H. (2006). Particle filtering and ensemble Kalman filtering for state updating with hydrological conceptual rainfall-runoff models. *Water Resources Research*, *42*, W09403. https://doi.org/10.1029/2005WR004093
Wooldridge, S. A., & Kalma, J. D. (2001). Regional-scale hydrological modelling using multiple-parameter landscape zones and a quasi-distributed water balance model. *Hydrological Earth System Sciences*, *5*, 59–74.

Young, P. C. (2002). Advances in real-time flood forecasting. *Philosophical Transactions of the Royal Society London*, *360*, 1433–1450.
Zaitchik, B. F., Rodell, M., & Reichle, R. H. (2008). Assimilation of GRACE terrestrial water storage data into a land surface model: Results for the Mississippi River basin. *Journal of Hydrometeorology*, *9*(3), 535–548. https://doi.org/10.1175/2007JHM951.1
Zhang, Y., Bocquet, M., Mallet, V., Seigneur, C., & Baklanov, A. (2012). Real-time air quality forecasting, Part I: History, techniques, and current status. *Atmospheric Environment*, *60*, 632–655.
Zhao, Y., Deng, X., Zhang, S., Liu, Z., Liu, C., Vecchi, G., et al. (2017). Impact of an observational time window on coupled data assimilation: Simulation with a simple climate model. *Nonlinear Processes in Geophysics*, *24*, 681–694. https://doi.org/10.5194/npg-24-681-2017